

Plasma Bubbles in the Post-Sunset Ionosphere

J.D. Huba,¹ G. Joyce², and J. Krall¹

¹ *Plasma Physics Division*

² *Icarus Research, Inc.*

Introduction: Post-sunset ionospheric irregularities in the equatorial F region were first observed by Booker and Wells¹ using high-frequency radio transmitters (ionosondes). This phenomenon has become known as equatorial spread F (ESF). During ESF, the equatorial ionosphere becomes unstable because of a Rayleigh–Taylor-like instability: large-scale (tens of km) electron density “bubbles” can develop and rise to high altitudes (1000 km or greater at times). Understanding and modeling ESF is important because of its impact on space weather: it causes radio wave scintillation that degrades communication and navigation systems. In fact, it is the focus of the Air Force Communication/Navigation Outage Forecasting System (C/NOFS) mission.

A major problem in self-consistently modeling equatorial plasma bubbles is capturing bubble dynamics on scale lengths of less than approximately 10 km within the context of the global ionosphere with scale lengths of approximately 1000s of km. This is critical because the day-to-day variability of ESF is controlled (in part) by the prereversal enhancement (PRE) of the eastward electric field. The PRE in turn is controlled by the thermospheric neutral wind through a global dynamo mechanism.

To meet the Navy’s need to specify the disturbed ionospheric environment, we have developed a new, three-dimensional code of the low- to mid-latitude

ionosphere that self-consistently models the onset and evolution of post-sunset, large-scale plasma bubbles in the equatorial ionosphere.

Results: Our initial effort to model equatorial plasma bubbles was based on a modified version of SAMI3, dubbed SAMI3/ESF.² SAMI3 is a comprehensive, 3D, first-principles physics model of the ionosphere developed at NRL; it is based on the NRL 2D model SAMI2.³ To achieve the high resolution (less than approximately 10 km) needed in the longitudinal (zonal) direction, we simulated a narrow “wedge” of the ionosphere in the post-sunset period. The angular width of the wedge was 4° (approximately 500 km), and the spatial resolution was approximately 5 km.

Although the plasma dynamics of the bubble was “decoupled” from the global electrodynamics of the ionosphere, we were able to model the 3D dynamics of equatorial bubble evolution for the first time. Figure 1 presents typical results from SAMI3/ESF simulations. This figure shows a 3D graphic of the electron density (left panel) and electron temperature (right panel). The large blue isosurface in the left panel is the rising plasma bubble associated with ESF. In the right panel, the blue isosurface shows the cooling of the electrons inside the bubble; the red isosurface shows the heating of the electrons by collisional coupling with the ions and by thermal conduction at higher altitudes. Subsequently we have used SAMI3/ESF to explain compositional anomalies, enhanced airglow, and “plasma blobs” associated with bubble development.

To overcome the limitation of SAMI3/ESF to a narrow longitudinal region of the ionosphere, we improved SAMI3 to self-consistently solve for the neutral wind-driven dynamo electric field as well as the gravity-driv-

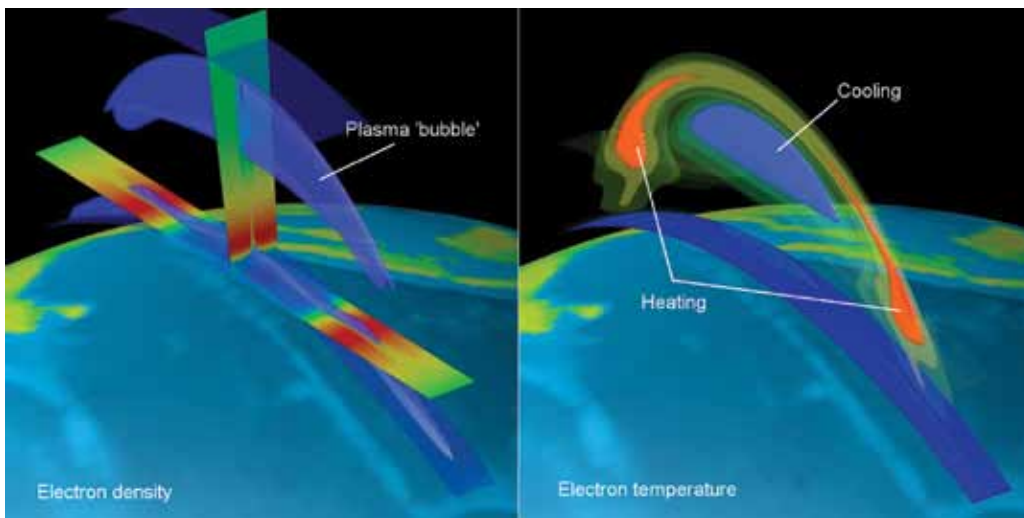


FIGURE 1 SAMI3/ESF simulation of an equatorial plasma bubble: electron density (left) and electron temperature (right).

en electric field associated with plasma bubbles.⁴ The latter is achieved by incorporating a high-resolution longitudinal grid in the pre- to post-sunset sector (i.e., 1630 MLT to 2230 MLT; MLT = magnetic local time). The minimum resolution in this region is $\Delta\phi = 0.0625^\circ$ (i.e., a spatial scale $\Delta x \sim 7$ km). Such high resolution in a global ionosphere model is unprecedented.

Initial results from the new version of SAMI3 are shown in Fig. 2. In this figure, we show color-coded contours of the electron density in the equatorial plane. The view is looking down on the Earth above the North Pole; the Sun is to the left, dawn is at the top and dusk is at the bottom. The ionosphere builds after sunrise, achieves a maximum density in the afternoon, and starts to decay after sunset. In this simulation, a 5% electron density perturbation is imposed in the F region (at 318 km) at magnetic local times 1700, 1720, 1740, 1800, and 1820. Note that sunset is at 1800 MLT, which is at the bottom of the figure. These perturbations convect into the post-sunset sector and initiate large-scale plasma bubbles (the dark blue tilted structures in the lower, right portion of the figure). These results are consistent with observational data.

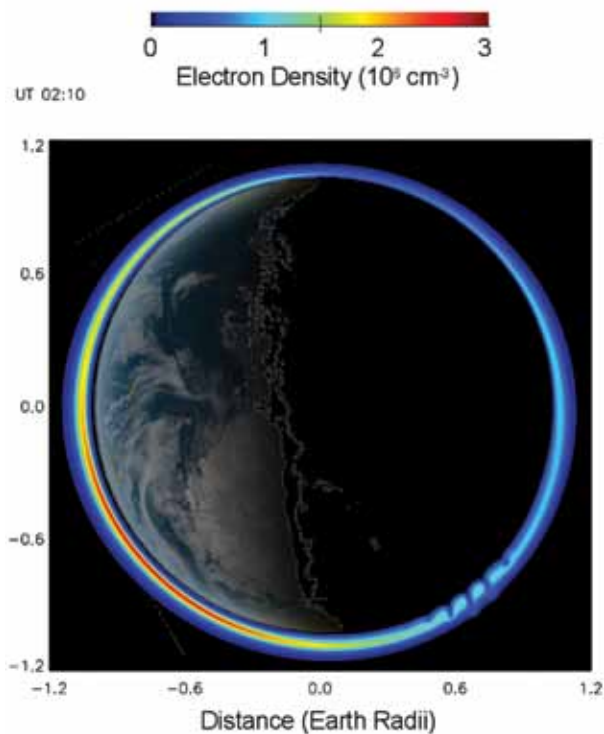


FIGURE 2
SAMI3 simulation equatorial plasma bubbles on a global scale.

Future Research: The upgraded version of SAMI3 represents a unique resource to investigate the physics of equatorial spread F. One vexing question concerning ESF is, what processes control the day-to-day vari-

ability of ESF? We will be able to address this question by investigating the impact of background ionospheric conditions on ESF bubble development (e.g., different neutral wind models, F10.7, PRE), as well as “seed” mechanisms such as gravity waves and velocity shear. To achieve closure, we will compare model results to data (e.g., radar measurements, optical observations, in situ satellite data) to assess the validity of the model results to explain ESF day-to-day variability.

[Sponsored by ONR]

References

- ¹ H.G. Booker and H.G. Wells, “Scattering of Radio Waves in the F-region of the Ionosphere,” *Terr. Mag. Atmos. Elec.* **43**, 249–256 (1938).
- ² J.D. Huba, G. Joyce, and J. Krall, “Three-dimensional Equatorial Spread F Modeling,” *Geophys. Res. Lett.* **35**, L10102 (2008), doi:10.1029/2008GL033509.
- ³ J.D. Huba, G. Joyce, and J.A. Fedder, “Sami2 is Another Model of the Ionosphere (SAMI2): A New Low-Latitude Ionosphere Model,” *J. Geophys. Res.* **105**, 23,035 (2000).
- ⁴ J.D. Huba and G. Joyce, “Global Modeling of Equatorial Plasma Bubbles,” *Geophys. Res. Lett.* **37**, L17104 (2010), doi:10.1029/2010GL044281.

The WISPR Instrument on the Solar Probe Plus Satellite

R.A. Howard, A. Vourlidas, S. Plunkett,
and C. Korendyke
Space Science Division

Introduction: Our Sun is 150×10^6 km away from Earth. This distance is called an astronomical unit (AU). All of our knowledge about the Sun originates from remote sensing instruments from the distance of the Earth or beyond and from in situ measurements of the solar wind, which is a constantly varying and very low-density plasma flowing out from the Sun. The closest that man has ever gone to the Sun is about 0.30 AU, which is the minimum distance of the planet Mercury in its orbit about the Sun.

The Sun itself is responsible for much of the variable nature of the solar wind, but there is a lot of interaction as the wind travels out to the vicinity of Earth’s orbit where most of the in situ observations have been made. How much of the variability that is seen at Earth is due to the source or due to the transport is an open issue. Even more important are a number of questions and assumptions about the near-Sun environment that have been lingering for 50 years, such as the following: What heats the corona? Are waves depositing energy in the corona, and if so, what type of wave? Or perhaps the energy comes from small coronal explosions, called

flares, driven by magnetic reconfigurations or some other mechanism? What accelerates the solar wind? What are the near-Sun plasma properties (particle density, magnetic field)? Does the solar wind come out in tubes that spread out? What is the thickness of the various plasma surfaces?

The National Aeronautics and Space Administration (NASA) is implementing a new mission to go close to the Sun in an encounter mode to answer these questions. Such an encounter mission was originally proposed in 1958 and has been proposed again several times since, but closely approaching the Sun demands new technology, particularly for heat rejection. The new NASA mission, Solar Probe Plus (SP+), will be launched in July 2018. NRL has been selected by NASA to provide the only imager for the mission. Our instrument, the Wide Field Imager for Solar Probe Plus (WISPR), will image the solar corona in white light. At its closest approach, SP+ will pass within about 5×10^6 km from the solar limb.

The Spacecraft: The spacecraft is a challenge to design: the spacecraft and instruments must be maintained at a relatively constant temperature, while the input energy flux onto the spacecraft increases to 510 times the value in Earth orbit. The Johns Hopkins University Applied Physics Laboratory (APL) is responsible for the SP+ spacecraft, shown in Fig. 3. Most of the instruments will sit behind the shadow of the thermal protection shield (TPS). The solar arrays generate electricity by converting the photons into electrical energy, but when the SP+ gets close to the Sun, the arrays must be stowed. Otherwise, the spacecraft is a normal 3-axis stabilized design. A high-gain antenna provides high-speed downlink when the spacecraft is more than 0.25 AU from the Sun. Low-gain antennas provide command uplink and “health and status” downlink during solar encounters.

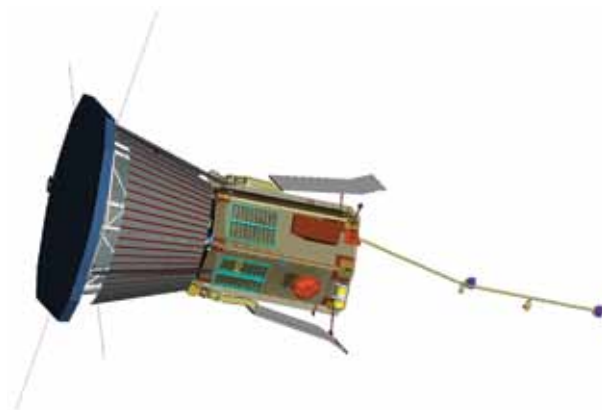


FIGURE 3 Solar Probe Plus spacecraft concept. The thermal protection shield is the hexagonal shaped plate at the top of the spacecraft and is always pointed at the Sun. It is fabricated with carbon-carbon sheets coated with a ceramic.

The Mission Profile: The SP+ will be put into an elliptic orbit using gravitational assists by flying close to the planet Venus to modify the orbit trajectory. Only three months after launch, the first perihelion of $35 R_{\text{sun}}$ ($1 R_{\text{sun}}$ is 696,000 km) is reached, and subsequent gravitational assists (a total of seven) lead to a minimum perihelion of $9.5 R_{\text{sun}}$ about 6.4 years (2025) after launch. The instruments will make observations for about 20 days (± 10 around each orbit perihelion). An orbit is about 90 to 100 days depending upon the perihelion. Figure 4 shows the distance profile as a function of time after launch.

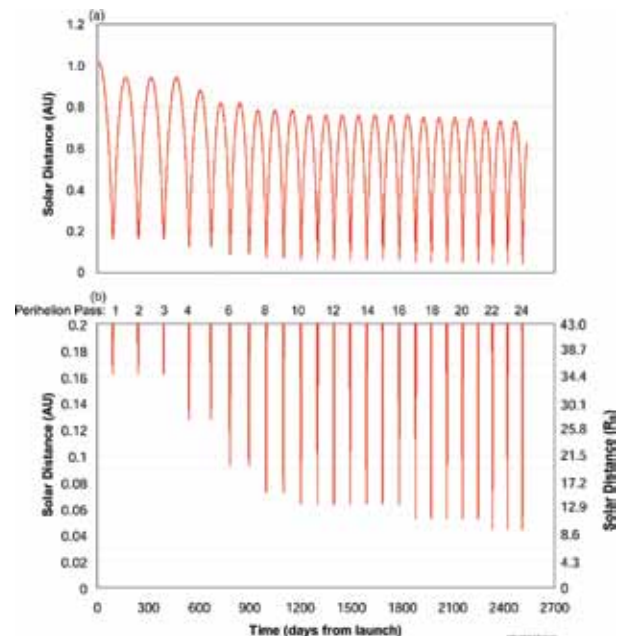


FIGURE 4 Solar distance profile of SP+. The upper plot shows both perihelion and aphelion, and the lower plot zooms in on the perihelion interval. The changes in the perihelion distances occur after each of the gravity assists resulting from the fly-bys of Venus.

The WISPR Instrument: WISPR images the solar corona with a 105° wide field of view, which corresponds to about $17 R_{\text{sun}}$ at the minimum perihelion distance of $9.5 R_{\text{sun}}$. The instrument observes in the visible and records the photospheric light scattered by the electrons within solar wind structures. This is very similar to the coronagraphs that NRL has flown on LASCO and SECCHI, but with much higher spatial resolution. As the spacecraft flies through the coronal density structures, they are first seen far away and then close up. Their substructure will be resolved to finer scales as they approach the spacecraft. At the same time, their scattering efficiency increases, making them easier to detect compared to solar wind structures further afield. This transition from remote sensing to local sensing will provide unprecedented observations of the

small-scale density fluctuations. The fast motion will also enable tomographic reconstructions from multiple viewpoints rather than just the two we have from the STEREO mission. If a coronal mass ejection (CME) occurs during the perihelion passage, SP+ will provide definitive measurements of the density and magnetic field ahead of and inside of the CME. WISPR will make the first observations of the dust-free region around the Sun, which has been a difficult, if not impossible, observation to make from 1 AU. Dust is the source of the zodiacal light or F-corona, but the dust evaporates as it nears the Sun. The distance at which the evaporation occurs depends on the particular material within the dust, which we expect to cause a slight inflection in the slope of the brightness curves.

WISPR will also search for density turbulence by taking images at a fast rate. Turbulence is a byproduct of wave heating. We will be able to explore the degree of turbulence in the near-Sun environment for various types of coronal structures beyond the local region around the spacecraft and to compare with the in situ measurements of magnetic and velocity turbulence.

The instrument, shown in Fig. 5, is a simple wide angle telescope, but with the complexity of rejecting the disk light by more than ten orders of magnitude to see the faint corona light. Our coronagraphic experience on the STEREO mission as well as previous missions carries over to this mission. Several new problems are presented and must be addressed. Both the dust and radiation environments will be greatly enhanced. The glass for the optics must survive impact of dust moving at a relative velocity of ~ 200 km/s and must be radiation hard. We must also replace the charge-coupled-device (CCD) sensors we have used previously with a new Advanced Pixel Sensor (APS) that is more immune to radiation damage. The APS opens up the new science

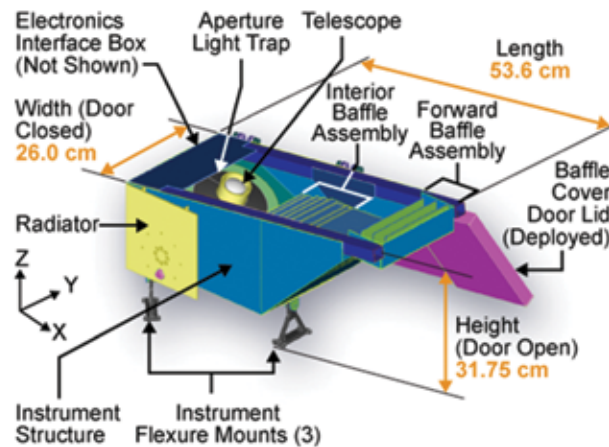


FIGURE 5
The WISPR instrument uses forward and interior baffles to reject unwanted scattered light from the Sun and the spacecraft. The concepts are derived from a significant heritage of coronagraphic instruments.

regime of turbulence studies from an imager because it allows fast readouts of selected regions of the detector. It accommodates variable exposure times across the field, which allows us to obtain high sensitivity across the full field of view despite the greater than 10^6 variation in the coronal signal.

Summary: The SP+ mission is an exciting mission with the promise of providing measurements of fundamental importance in solving some of the major outstanding problems of solar physics. The Space Science Division–provided WISPR instrument, the only imager on board, plays a fundamental role in the success of this mission. WISPR will provide the first close-up images of the solar wind, coronal mass ejections, and possibly sungrazer comets. It will finally verify whether a dust-free zone exists in the inner corona. The WISPR images and density spectra link the remote sensing observations of the solar corona (from other platforms) and the in situ measurements from the SP+ payload, thus ensuring that the long-standing secrets of the solar wind will finally be revealed.

[Sponsored by NASA]

Solar Active Regions – The Sources of Space Weather

G.A. Doschek and H.P. Warren
Space Science Division

The Magnetic Sun and Solar Activity: In visible light, the Sun appears as a near-constant light source that varies significantly in brightness only over time-scales of millions of years. The Sun in visible light is a relatively normal and not too interesting star compared with the zoo of astronomical objects such as supernova explosions and black holes. However, when solar radiation other than visible light is examined, the story changes dramatically. Two-thirds of the way from the Sun's core to its surface, convection of the solar gas begins and a magnetic dynamo is generated. Magnetic fields contain energy, and the fields disrupt the flow of radiative energy from the Sun's core to its surface, producing cool regions called sunspots. The magnetic fields near the sunspots are strong and, together with surrounding weaker fields, turn the Sun into an enormous magnetic object with an extremely complicated magnetic structure (see Fig. 6).

By processes not yet understood, the gas above the Sun's surface is heated by this magnetic field to temperatures ranging from 10,000 K to between 3 and 4 million degrees, creating a vast atmosphere that flows outward (the solar wind) past the Earth to the very

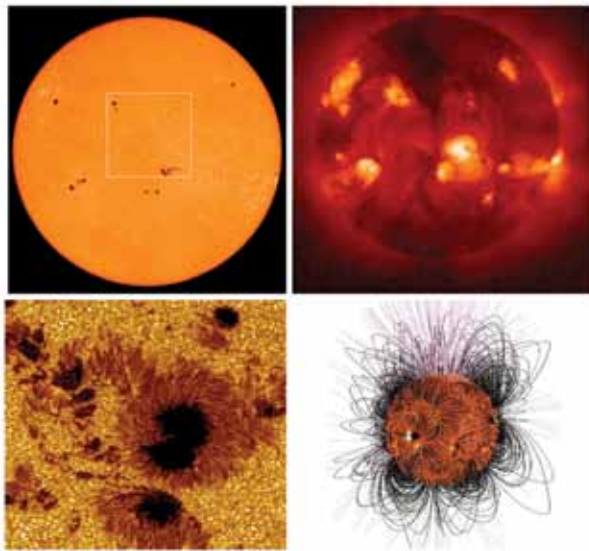


FIGURE 6
 Upper left: visible light image of the Sun showing sunspots. Upper right: image of the Sun in X-rays showing hot bright regions above sunspots. Lower left: a sunspot up close showing surrounding convective “granules.” Lower right: the Sun’s magnetic field extending up into the solar atmosphere.

edge of the solar system, where it plows into the interstellar medium. The ultraviolet (UV), extreme-ultraviolet (EUV), and X-rays from the Sun are enormously variable, and sometimes the magnetic fields twist and annihilate themselves (by a process called magnetic reconnection), converting their energy into titanic explosions called flares and coronal mass ejections (CMEs). Flares reach temperatures of 30 million degrees and more, and a CME can send a billion tons of matter moving towards Earth at a million miles an hour. The X-ray–UV radiation and energetic particles in these eruptions create hazards to DoD assets in space, forming a local space weather that must be predictable in order to protect those assets.

The hottest regions of the Sun’s atmosphere, and the regions in which flares and CMEs occur, are located over sunspots and are called active regions because they are seething infernos of transient eruptions and explosions. The gas in active regions is confined to magnetic lines of force and appears as giant plumes and loops. Understanding the heating in these linear structures is critical for understanding the flares and CMEs that are initiated in active regions.

Understanding Solar Activity at NRL: At NRL there is a sophisticated space-based remote sensing program working towards understanding the causes of active region heating with extensive support from NRL/ONR and NASA. One of our instruments is an Extreme-ultraviolet Imaging Spectrometer (EIS) flown on a Japanese spacecraft called Hinode. This instru-

ment is an international collaboration involving the U.S., the UK, Norway, and Japan. A spectrometer breaks light down into its component wavelengths (colors). Different elements such as iron emit radiation at discrete wavelengths (“spectral lines”) depending on how many electrons are present around the atom’s nucleus, and this depends on the temperature. EIS detects these spectral lines, and from atomic physics we can decipher the information they contain. Thus, EIS is a remote sensing thermometer, and by comparing the spectral lines of the same and different elements, it can also function as a barometer, a chemical composition analyzer, and, perhaps best of all, measure the speeds and turbulence in the gas within and above the active regions.

Heating and Dynamics of the Solar Atmosphere:

With the unprecedented diagnostic information provided by EIS, we are finally beginning to understand the characteristics of the physical processes that actually heat the loops,¹ and as the current solar cycle proceeds to solar maximum, we hope to apply our techniques to understanding flares and mass ejections. For example, we find that the cores of active regions contain very hot loops with temperatures of 3 to 4 million degrees, while the outer parts of active regions contain “warm” loops with temperatures of about 1.4 million degrees. Figure 7 shows an active region as it appears in spectral lines formed at different temperatures. We find that the hot core loops appear to be steadily heated, while the warm loops are transiently heated. We are linking the heating characteristics of loops to the magnetic field structure of the active region, thus advancing our understanding of how magnetic energy is converted to gas heating.

Another interesting result concerns the length of time it takes the warm loops to cool. From intensity light curves and density measurements made with EIS, we now know that the warm active region loops contain unresolved magnetic structures that are somehow heated and cooled coherently. The density measurements imply that the loops should have much shorter lifetimes than observed. We can explain the observed lifetimes with a model that sequentially heats unresolved magnetic threads in the loops. However, the temperature evolution of the loops indicates that the sequential heating is not in complete agreement with the idea that the heating is caused by very tiny flares, called nanoflares, that is currently a popular model.

Finally, at the edges of active regions we find extended outflow regions (see Fig. 8) with plasma flowing outward at speeds ranging from 50 to 200 km/s.² We feel that at least some of this outflowing plasma reaches the heliosphere and could form part of the slow solar wind. EIS is revealing new and exciting results from

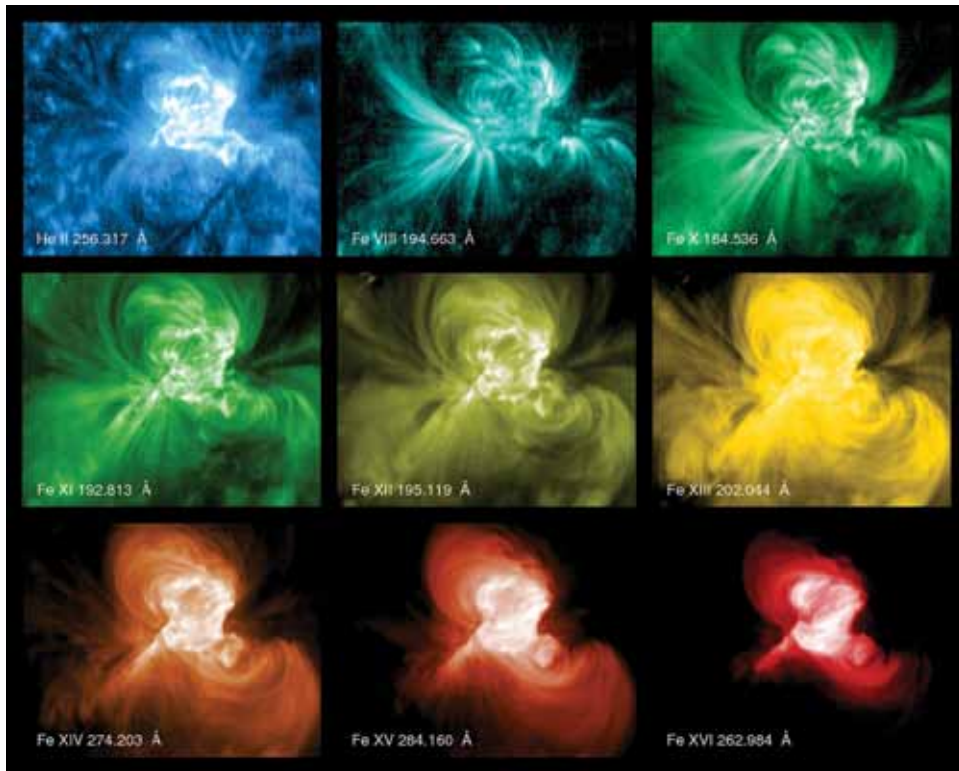


FIGURE 7
An active region as it appears in spectral lines of helium and iron formed at temperatures ranging from about 100,000 degrees (upper left) to 3–4 million degrees (lower right). Images from Hinode/EIS.

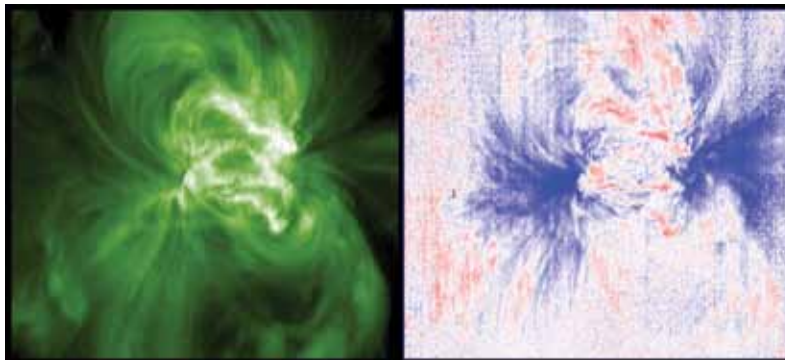


FIGURE 8
Left: An active region image in a spectral line of Fe XII formed at about 1.4 million degrees. Right: a Doppler map showing gas flow in the active region towards us (blue) and away from us (red). White emission corresponds to no velocity along our line of sight. Images from Hinode/EIS.

active regions, taking us closer to understanding how active regions are heated and produce transient phenomena. This brings us closer to realizing a predictive space weather capability based on the actual physics that produces space weather.

[Sponsored by NRL and ONR]

References

- ¹ H.P. Warren, D.M. Kim, A.M. DeGiorgi, and I. Ugarte-Urra, “Modeling Evolving Coronal Loops with Observations from STEREO, Hinode, and TRACE,” *Astrophys. J.* **713**, 1095–1107 (2010).
- ² P. Bryans, P.R. Young, and G.A. Doschek, “Multiple Component Outflows in an Active Region Observed with the EUV Imaging Spectrometer on Hinode,” *Astrophys. J.* **715**, 1012–1020 (2010).

Testing Spacecraft Atomic Clocks

F.M. Vannicola, R.L. Beard, J.D. White, K.L. Senior, A.J. Kubik, and D.C. Wilson
Space Systems Development Department

Introduction: NRL is conducting the third in a series of Global Positioning System (GPS) atomic frequency standard life tests in the NRL Precision Clock Evaluation Facility (PCEF). The PCEF is one of the major facilities within the Naval Center for Space Technology and an overview is provided in the *2008 NRL Major Facilities* book. Figure 9 is a block diagram of the PCEF. The PCEF was originally developed to evaluate high precision atomic clocks for the GPS concept program (Block I). The facility was expanded for dedicated space clock evaluation conducted for operational system development and deployment. The space atomic clocks' progress is evaluated, and the clocks are qualified and acceptance-tested for space flight using the facility's assets. Testing performed includes long- and short-term performance evaluation and environmental testing (including shock and vibration). Investigations of on-orbit anomalies are performed within the PCEF

in an attempt to duplicate and understand similar effects in space-qualified hardware under controlled conditions. The ability to evaluate and test highly precise atomic clocks, especially in a space environment, requires unique facilities, precise time and frequency references, and precise instrumentation not available elsewhere.

Background: The first extended life test conducted at NRL was on the GPS Block IIR Rubidium Atomic Frequency Standard (RAFS), which began in 1997 and lasted more than seven years.¹ Each Block IIR satellite contains three RAFS units. That life test began about one year before any of the RAFS were used in orbit. For the GPS Block IIF program, each satellite will contain one Digital Cesium Beam Frequency Standard (DCBFS) manufactured by Symmetricom, and two Rubidium Frequency Standards (RFS) built by PerkinElmer Optoelectronics. Life testing of two DCBFS flight production units began in August 2004 and has been on hold since October 2006 due to DCBFS production parts availability problems; however, these tests will resume in FY 2011. The third life test, which involves two production RFS units, has run continuously since August 22, 2008. The Block IIF life test is being con-

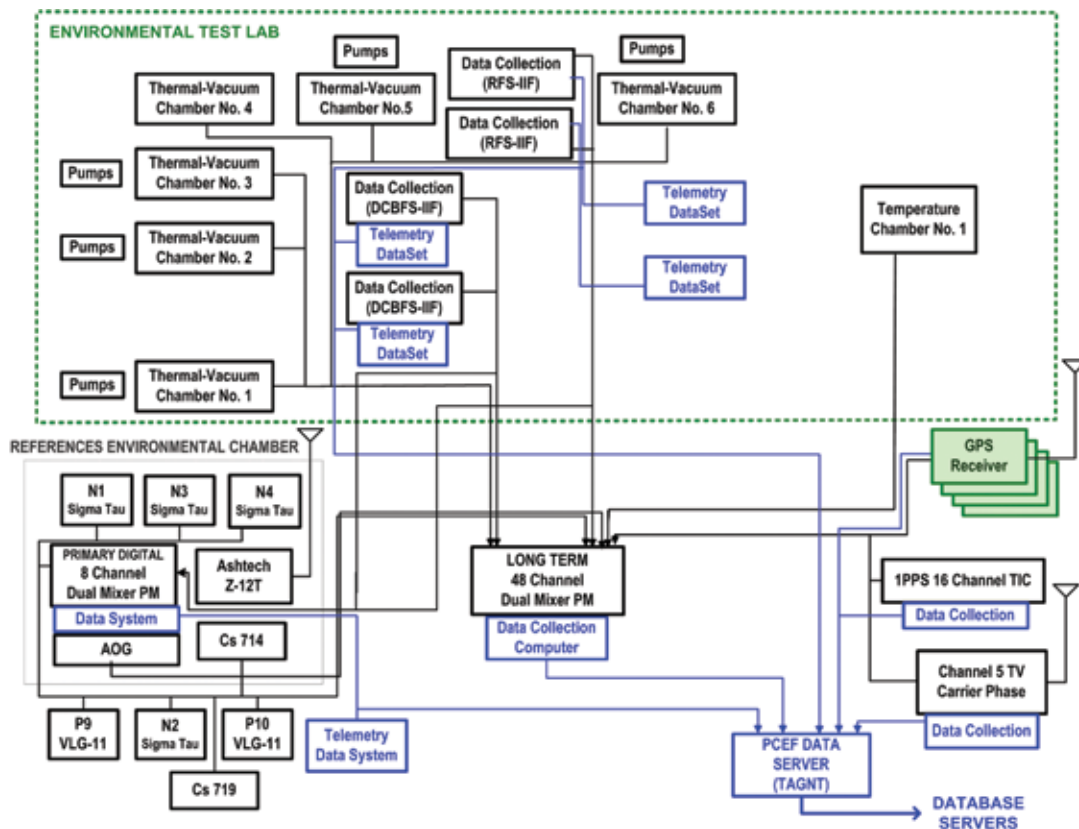


FIGURE 9 The NRL PCEF consists of the Time and Frequency References, Precision Clock Signal Measurement Systems, Environmental Testing Laboratory, Data Systems and Server, and GPS Receiver Laboratory.

ducted in conjunction with the GPS Directorate, GPS Block IIF Prime Contractor, Boeing, and the atomic frequency standards manufacturers, and is scheduled to run for a minimum of 3 years.² With the launch of the first GPS Block IIF satellite on May 28, 2010, NRL gained the unique ability to compare the ground clock performance with the clocks on-orbit. The frequency stability performance requirement for the GPS Block IIF clocks is 6×10^{-14} at one day.

Life Test Configurations: The life test principal objectives are accomplished by evaluating each Block IIF flight unit under continuous operation in a simulated space-like environment, thus replicating their operation in the GPS spacecraft as closely as possible. Separate thermal vacuum chambers whose mounting baseplates are independently temperature controlled house each of the units (Fig. 10). Figure 11 is a schematic diagram of the RFS life test configuration, which is similar to the DCBFS setup.



FIGURE 10
One of the closed vacuum chambers and equipment racks containing the data collection and monitoring systems.

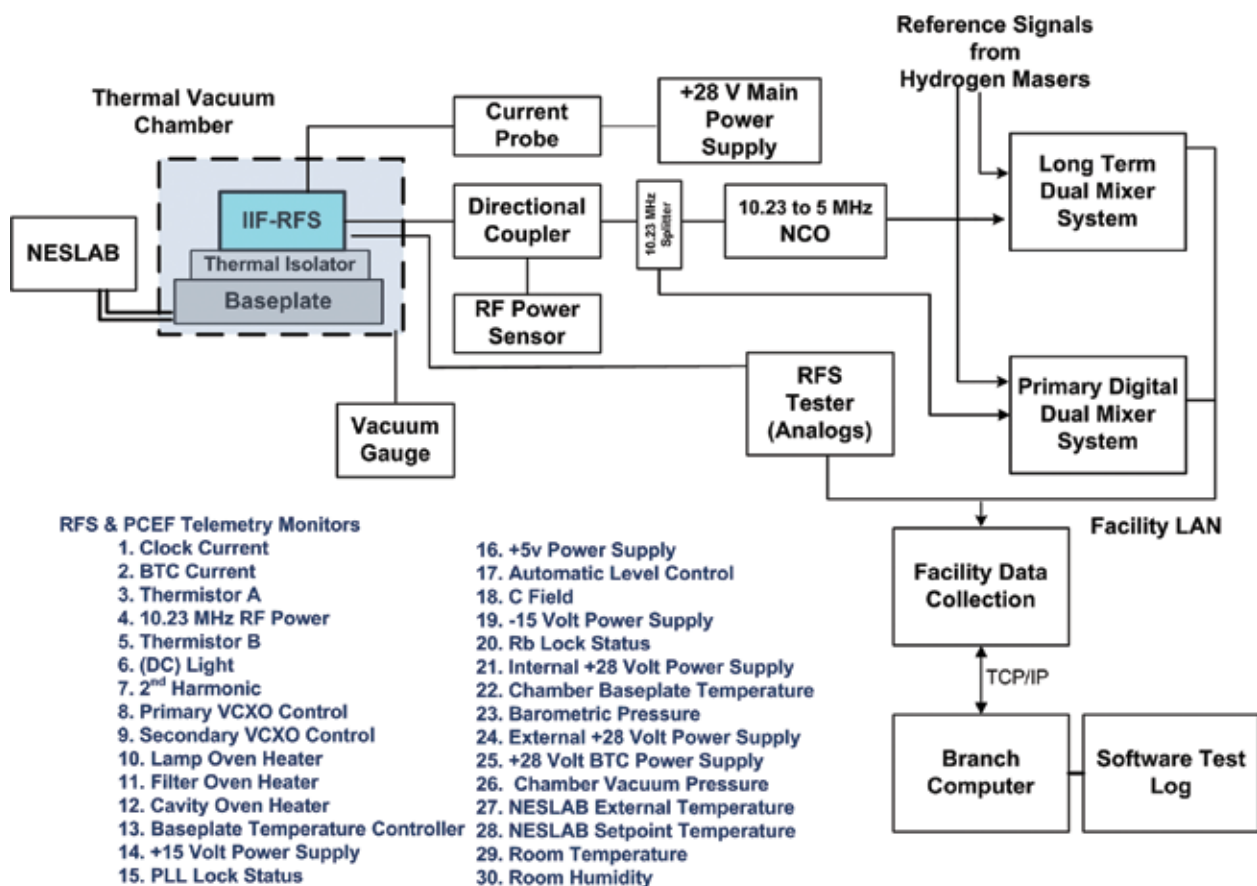


FIGURE 11
RFS life test configuration and list of clock telemetry and PCEF environmental monitors.

DCBFS Anomalies/Performance: The DCBFS life test quickly uncovered a defect in the high voltage power supplies used for the ion pump and electron multiplier functions in the clocks. The first unit failed approximately 100 days into the test and after repair failed again 21 days into operation. The other unit had a continuous run of 591 days before it too experienced the same failure. The power supply problem was thoroughly researched and the flight units were modified to prevent future failures. No other anomalies were found.

RFS Anomalies/Performance: There have been no failures associated with either RFS unit; however, both units have experienced a combined total of 10 frequency steps, which were also seen during the RAFS life test and on-orbit. The steps experienced have ranged between -3.5×10^{-14} and $+7 \times 10^{-14}$. Neither clock is exhibiting a pattern to these steps. On two occasions there was an apparent correlation between the telemetry and the frequency steps. Clocks of this type have a tendency to experience frequency jumps, and specific causes have yet to be determined.

Temperature Testing: In an attempt to replicate the temperature changes experienced on board a GPS satellite, temperature cycling of one RFS unit was performed using the ± 3.5 °C peak-to-peak 12-hour cycle requirement from the clock specification. Effects were seen throughout the clock parameters, and the most notable, as expected, are in the baseplate thermal controller and the various ovens. Additional testing is required to determine a temperature coefficient.

Relevance: The NRL PCEF is a unique facility that provides the ability to perform extended life tests in order to establish a baseline for on-orbit clock performance and to identify potential risks in the flight test units. After 2 years of continuous operation, the two RFS life test units are performing well and display excellent stability. Despite the anomalies experienced in the two DCBFS life test units, their stabilities performed within design limits. With the launch of the first Block IIF satellite, the on-orbit performance of both the DCBFS and RFS clocks is within specification.

[Sponsored by the GPS Directorate]

References

- ¹ R. Beard, J. Buisson, F. Danzy, M. Largay, and J. White, "GPS Block IIR Rubidium Frequency Standard Life Test Results," in Proceedings of the 2002 IEEE International Frequency Control Symposium, May 29–31, 2002, New Orleans, Louisiana, pp. 449–504 (2002).
- ² F. Vannicola, R. Beard, J. White, K. Senior, A. Kubik, and D. Wilson, "GPS Block IIF Rubidium Frequency Life Test," in Proceedings of the Institute of Navigation Global Navigation Satellite System Conference, September 21–24, 2010, Portland, Oregon, pp. 812–819 (2010). ■